

# An Approach for Designing Patient-specific Prosthetic Aortic Valves Based on CTA Images Using Fluid-structure Interaction (FSI) Method

Yingyi Geng<sup>1</sup>, Yue Wang<sup>2</sup>, Yanqiong Ye<sup>2</sup>, Zhenyin Fu<sup>1</sup>, Dongdong Deng<sup>3</sup>, Yanqiu Feng<sup>4</sup>, Wufan Chen<sup>4</sup>, Ling Xia<sup>1</sup>

<sup>1</sup> Key Laboratory for Biomedical Engineering of Ministry of Education, Institute of Biomedical Engineering, Zhejiang University, Hangzhou, China

<sup>2</sup> Department of Cardiac surgery, School of Medicine, Sir Run Run Shaw Hospital, Zhejiang University, Hangzhou, China

<sup>3</sup> School of Biomedical Engineering, Dalian University of Technology, Dalian, China

<sup>4</sup> School of Biomedical Engineering, Southern Medical University, Guangzhou, China

## Abstract

*Background:* Currently, the efficacy of prosthetic valves is highly dependent on the geometry of the aortic root. With the development of computational fluid dynamics, patient-specific modeling and simulation of prosthetic heart valves increasingly become the forefront of current research. *Methods:* In this study, we propose an approach for designing patient-specific prosthetic aortic valves using fluid-structure interaction (FSI) analysis. Firstly, the aortic root model was reconstructed from the computed tomography angiography (CTA) images. We then implemented a parametric valve design. The leaflets were determined by the attachment curve, the free edge, and the belly curve. We selected six key points, including three points located at the ends of the free edge, and three points located at the bottom of the attachment curve. This allowed for designing various leaflet geometries. Furthermore, each valve model was simulated using the FSI method. We evaluated deformation, effective orifice area (EOA), and stress to study its performance. *Conclusion:* The simulation results showed that patient-specific valves demonstrated a large EOA and proper stress, indicating satisfactory performance. Our study investigated an approach for designing patient-specific prosthetic aortic valves and evaluated hemodynamic parameters. This provides promising insights into the design of prosthetic aortic valves and potentially serves as a valuable tool to assist patient-specific aortic valve replacement.

## 1. Introduction

Valvular heart diseases refer to the structural or

functional abnormalities of the heart valves, which can severely affect the normal function of the heart. Aortic valve diseases account for a relatively high proportion of valvular heart disease, while its primary treatment method is surgical aortic valve replacement [1]. Currently, mechanical heart valves and bio-prosthetic heart valves have been greatly popularized and applied all over the world. Compared with mechanical heart valves, bio-prosthetic heart valves show better tissue compatibility and hemodynamic performance [2]. In recent years, some clinicians have been dedicated to exploring new surgical approaches for aortic valve diseases. Significantly, the reconstructive surgery called AVNeo (Aortic Valve Neocuspidization) procedure, proposed by Ozaki in Japan, has shown excellent clinical efficacy [3]. However, there exist variations in the aortic valve geometry among different patients, which can significantly impact the opening and closing functionality of the aortic valve [4]. In consequence, it is of importance to design the individual prosthetic aortic valves (PAV) based on the patient-specific aortic root geometry.

The advancement of computer simulations of fluid and mechanics has significantly contributed to the progress in the field of heart valve research. Zakerzadch et al. summarized the latest advancements in computational methods for aortic valves, including geometric modeling, material modeling of the leaflets, and simulation techniques [5]. This study suggests that the improvements in bio-prosthetic heart valve design can have a dramatic clinical impact. Feng's research demonstrated the clinical effectiveness of aortic valve reconstructive surgery based on patient-specific computed tomographic angiography (CTA) images and immersed boundary method (IBM), while a uniform leaflet model was used in this study [6]. Xu et al. proposed a framework for the parametric design

of valve leaflets based on patient-specific aortic root models [7]. This innovative approach has yielded valuable insights into bioprosthetic heart valve design, additionally, the parametric method of valve geometry can be further optimized.

In this study, we developed a novel parametric approach for designing the aortic valve leaflets, extracting coordinates from CTA images to define key points that determine the shape of leaflets. Then by defining the valve leaflet parameter equations, we have successfully generated patient-specific leaflets. Subsequently, simulation modeling was performed to evaluate its performance and functionality.

## 2. Materials and Methods

### 2.1. Patient-specific Aortic Root Model

We selected a patient with a normal aortic root structure and collected the patient-specific cardiac CTA images, which were obtained from Sir Run Run Shaw Hospital of Zhejiang University School of Medicine. The three-dimensional (3D) geometric model of the aortic root was reconstructed from the CTA images using the MIMICS 18.0 (Materialise N.V., Belgium). The smoothing process was applied to mitigate the impact of noise and artifacts in the CTA images. Subsequently, the coordinates of six critical locations were obtained by combining the CTA images and the 3D model, including the attachment points ( $P_{k1} - P_{k3}$ ) at the sinotubular junction and the basal attachment points ( $P_{k4} - P_{k6}$ ) of the valve leaflets, as illustrated in Table 1 and Figure 1.

Table 1. The Coordinates of key points ( $P_{k1} - P_{k6}$ )

Point	Coordinate
$P_{k1}$	(0.2050, -158.330, -739.845)
$P_{k2}$	(-10.425, -177.724, -750.616)
$P_{k3}$	(7.5638, -177.094, -731.568)
$P_{k4}$	(13.148, -183.160, -752.934)
$P_{k5}$	(5.8786, -164.926, -763.128)
$P_{k6}$	(21.528, -165.601, -744.954)

### 2.2. Parametric PAV design

A normal aortic valve consists of the left coronary leaflet, right coronary leaflet, and non-coronary leaflet, whose shapes are highly dependent on the geometry of the patient-specific aortic root [8]. Based on Haj-Ali et al's work [9], we defined three parametric curves, namely the attachment curve, the belly curve, and the free edge, as shown in Figure 1(c), to describe the shape of the aortic valve leaflet. In previous studies, it was common to

define curves using a cylinder within the (x, y, z) coordinate system. However, in this study, the 3D model of the aortic root already had coordinate values. Therefore, we utilized the coordinate values and the relative position of key points ( $P_{k1} - P_{k6}$ ) to define the parameter curves of the leaflets.

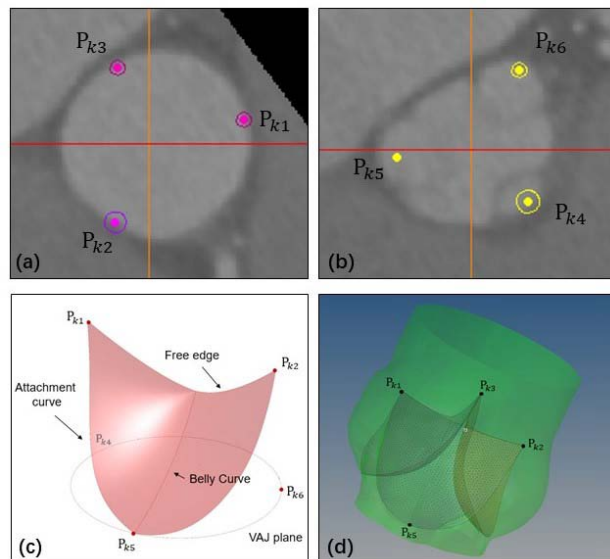


Figure 1. (a) (b): Positions of key points; (c): Parametric of the valve leaflet; (d): 3D model of the aortic root and valve leaflets.

Initially, the STJ plane was constructed using the coordinates of  $P_{k1}$ ,  $P_{k2}$ , and  $P_{k3}$ . The intersection point between the free edge and the belly curve was referred to as the TopPoint. The coordinates of the TopPoint were influenced by the effective height of the leaflet and the gap at the center of the leaflets. The belly curve, a quadratic Be'zier curve, was then defined by three control points, determining the effective height of the valve leaflet. The formula for the belly curve was the following:

$$B(t) = (1 - t)^2 P_0 + 2(1 - t)t P_1 + t^2 P_2 \quad (1)$$

where  $t \in [0, 1]$ ,  $P_0$  and  $P_2$  are the hinge attachment point and TopPoint, respectively. The coordinates of  $P_1$  depended on the curvature, thus the detailed coordinate can be calculated by referring Fig 2(a).

The free edge was constructed simultaneously based on two projection lines. One was the projection of B-splines on STJ plane. This curve met the following expressions:

$$x = f(y) = g + \alpha y^n \quad (2)$$

where  $g$  was the gap at the center of the leaflets,  $\alpha = (R_{OP} \cos \theta - g) / (R_{OP} \sin \theta^n)$ ,  $n \in [1.2, 1.7]$ . Specifically, the definition of  $R_{OP}$  and  $\theta$  is shown in Figure 2.

Furthermore, another construction line was the projection of B-splines onto the plane, which passed through the TopPoint and was perpendicular to the

symmetrical surface of the leaflet. We proposed the following expression:

$$y = f(x) = -H_f + \beta x^m \quad (3)$$

where  $H_f$  was the distance from TopPoint to the STJ plane,  $\beta = H_f/R_{OP}^m$ ,  $m \in [1.2, 1.7]$ .

The attachment curve determined how the valve leaflet attached to the sinus. In patient-specific valve design, it was essential for the attachment curve to align with the geometry of the aortic root. Consequently, we manually selected points on the aortic root model surface and interpolated them to the B-spline curve. The parametric design of the valve leaflet curve was implemented using Rhino and Grasshopper, as the results are shown in Figure 1(c) and Figure 1(d).

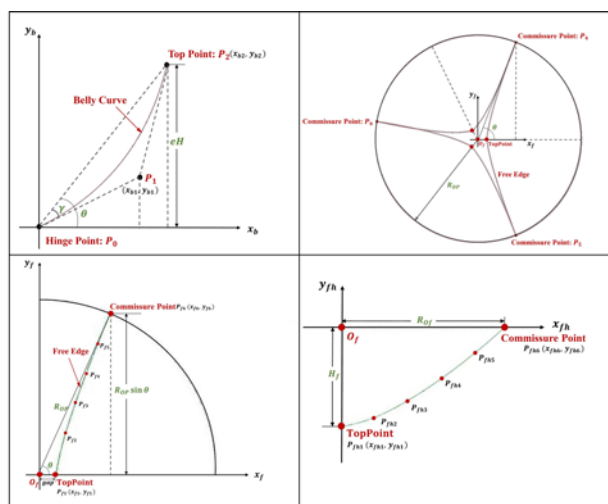


Figure 2. Design variables and control points for the generation of the belly curve and free edge. eH: effective height.

### 2.3. Model processing and FSI simulation

The left coronary leaflet, right coronary leaflet, and non-coronary leaflet were designed, respectively. Subsequently, the parametric curves were rebuilt to approximate the natural shape of the leaflets. The surfaces were filled using Matlab software. By varying the effective height (eH) and curvature, we were able to generate different valve leaflet models. To reduce computing time, we evaluated the performance of a valve with an effective height of 12 mm and a commissure angle of 30 degrees. In this study, we employed the incompressible computational fluid dynamics (ICFD) solver to deal with the flow-structure interaction between the aortic root and the valve leaflets. The ICFD solver is capable of conducting highly FSI analyses, which is well-suited for investigating the strong deformation of leaflets.

In the structural domain, the leaflets were considered

to be the hyperelastic material, using the Ogden 2nd order model [10, 11]. The attachment curve of the leaflet model was fixed to restrict its degrees of freedom in the X, Y, and Z directions. We assumed that the three leaflets have frictionless contact and strong deformations, selecting implicit dynamic analysis. In the fluid domain, the blood was defined as a Newtonian fluid with a density of 1050 kg/m<sup>3</sup> and a viscosity of 0.00035 Pa·s [12]. The ventricular pressure was implemented as the inlet boundary condition, while the physiological pressure corresponding to the aortic pressure was applied to the outlet boundary condition [6]. Additionally, on the vessel walls, the non-slip assumption was used. The time step was set to 0.1 ms for the ICFD solver. The cardiac cycle was set to be 0.85 s, we evaluated the motion and physiological states of the aortic valve in one cardiac cycle. The simulation was performed using the software LS-DYNA.

## 3. Result

### 3.1. Leaflet deformation and EOA

Figure 3 illustrates the deformation of the leaflets over one cardiac cycle. There are some significant points to describe the opening behavior of the leaflets. The leaflets start to open at 0.03 s, nearly fully open at 0.09 seconds, begin to close at 0.2 s, and reach partial close at 0.25 s, finally, achieve complete close at 0.3 seconds. During the diastolic phase, as the aortic pressure is significantly higher than the ventricular pressure, the leaflets will completely close. The effective orifice area (EOA) is an important parameter, representing the actual aortic valve aperture. Using the Gorlin formula [7], the EOA can be up to 3.42 cm<sup>2</sup>.

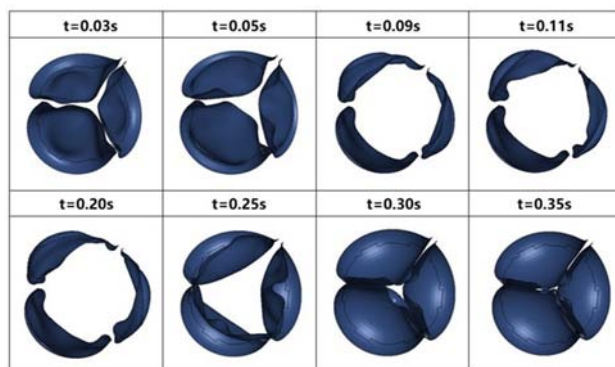


Figure 3. The deformation of the valve leaflets over one cardiac cycle.

### 3.2. Leaflets Stress and Strain

Figure 4 shows the maximum principal stress distributions of aortic valve leaflets in a cardiac cycle.

During the systolic phase, the heart propels blood into the aorta, resulting in relatively lower stress and pressure on the valve leaflets. However, with the impact force and the increase of flow velocity, the stress on the leaflets surface also correspondingly increases. During the diastolic phase, the valve leaflets rapidly close, leading to a significant increase in stress and strain.

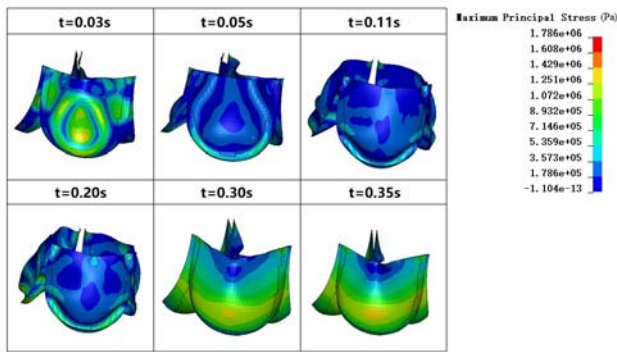


Figure 4. The maximum principal stress distributions of aortic valve leaflets in a cardiac cycle.

#### 4. Discussion and Conclusions

This study proposed an approach for designing patient-specific prosthetic aortic valves based on CTA images. The 3D model of the aortic root was reconstructed and the coordinates of key points were extracted, subsequently, the free edge, the belly curve, and the attachment curve were generated based on the parametric equations. This method also allows for the adjustment of parameters such as effective height and curvature to generate different shapes of valve leaflets. Through fluid-structure interaction simulations, the valve leaflets demonstrated large EOA and stress performance, confirming the effectiveness of this approach.

In current clinical practice, aortic valve replacement surgery commonly relies on standardized valve molds of specific sizes. However, with the progress of individual medicine, there is an exciting prospect of designing patient-specific valve leaflets based on the CTA image data. By FSI simulations, we aim to provide valuable support for optimizing the design of patient-specific valve leaflets.

#### Acknowledgments

This work was supported by the National Natural Science Foundation of China (62171408).

The authors declare there is no conflict of interest.

#### References

[1] Coffey S, Cairns BJ, Iung B. "The modern epidemiology of heart valve disease," *Heart*, vol. 102, no. 1, pp. 75–U5, Jan,

2016.

[2] Taylor J. "ESC/EACTS guidelines on the management of valvular heart disease cardiologists and surgeons have joined forces to write the valve guidelines for the first time," *European Heart Journal*, vol. 33, no. 19, pp. 2371–2372, Oct, 2012.

[3] Ozaki S, Kawase I, Yamashita H, Uchida S, Nozawa Y, Takatoh M, Hagiwara S. "A total of 404 cases of aortic valve reconstruction with glutaraldehyde-treated autologous pericardium." *Journal of Thoracic and Cardiovascular Surgery*, vol. 147, no. 1, pp. 301–306, Jan, 2014.

[4] Marom G, Haj-Ali R, Rosenfeld M, Schaefer HJ, Raanani E. "Aortic root numeric model: Annulus diameter prediction of effective height and coaptation in post-aortic valve repair," *Journal of Thoracic and Cardiovascular Surgery*, vol. 145, no. 2, pp. 406–U439, Feb, 2013.

[5] Zakerzadeh R, Hsu MC, Sacks MS. "Computational methods for the aortic heart valve and its replacements," *Expert Review of Medical Devices*, vol. 14, no. 11, pp. 849–866, Dec, 2017.

[6] Feng Y, Cao Y, Wang W, Zhang H, Wei L, Jia B, Wang S. "Computational modeling for surgical reconstruction of aortic valve by using autologous pericardium," *Ieee Access*, vol. 8, pp. 97343–97352, Jul, 2020.

[7] Xu F, Morganti S, Zakerzadeh R, Kamensky D, Auricchio F, Reali A, Hughes TJR, Sacks MS, Hsu MC. "A framework for designing patient-specific bioprosthetic heart valves using immerse geometric fluid-structure interaction analysis," *International Journal for Numerical Methods in Biomedical Engineering*, vol. 34, no. 4, Ari, 2018.

[8] Hammer PE, Berra I, del Nido PJ. "Surgical repair of congenital aortic regurgitation by aortic root reduction: A finite element study," *Journal of Biomechanics*, vol. 48, no. 14, pp. 3883–3889, Nov, 2015.

[9] Haj-Ali R, Marom G, Zekry SB, Rosenfeld M, Raanani E. "A general three-dimensional parametric geometry of the native aortic valve and root for biomechanical modeling," *Journal of Biomechanics*, vol. 45, no. (14), pp. 2392–2397, Sep, 2012.

[10] Castravete S, Mazilu D, Gruionu LG, Militaru C, Militaru S, UdriStoiu AL, Iacob AV, Gruionu G. "Finite element analysis of a novel aortic valve stent," *Current health sciences journal*, vol. 46, no. 3, pp. 290–296, Jul, 2020.

[11] Gao B, Zhang Q, Chang Y. "Hemodynamic effects of support modes of lvads on the aortic valve," *Medical & Biological Engineering & Computing*, vol. 57, no. 12, pp. 2657–2671, Nov, 2019.

[12] Geng Y, Liu H, Wang X, Zhang J, Gong Y, Zheng D, Jiang J, Xia L. "Effect of microcirculatory dysfunction on coronary hemodynamics: A pilot study based on computational fluid dynamics simulation," *Computers in Biology and Medicine*, vol. 146, Jul, 2022.

Address for correspondence:

Ling Xia  
38 Zheda Road, Hangzhou 310027, China.  
xialing@zju.edu.cn